

The Topological Origin of Bohm Resistivity in Magnetic Reconnection

Magnus F Ivarsen*

Department of Physics and Engineering Physics, University of Saskatchewan, Saskatoon, Canada

The physical origin of ‘anomalous’ resistivity in magnetic reconnection remains one of the longest-standing problems in space plasma physics. While the empirical Bohm diffusion scaling ($\eta \propto T/B$) is widely invoked to explain fast reconnection rates, it lacks a rigorous derivation from first principles. Here, we derive this scaling by modeling the magnetized electron fluid as an overdamped spintronic condensate governed by the Landau-Lifshitz-Gilbert equation. We demonstrate that the breakdown of the “frozen-in” condition is rigorously identified as an Adler-Ohmic bifurcation in the model: a topological phase transition where electron gyro-axes lose synchronization with the magnetic field. By rigorously mapping the breakdown of adiabatic invariance to electron gyro axis slippage on the unit sphere, we show that the resulting resistivity naturally saturates at the Bohm limit. Numerical simulations of the XY universality class confirm that the onset of this resistive state is explosive, following a logistic trigger consistent with the impulsive phase of solar flares. Furthermore, the topological defects in the condensate decay via a $t^{-0.75}$ power law, consistent with magnetic island coalescence as the mechanism of anomalous transport. These results suggest that Bohm resistivity is a universal topological property of magnetized matter at the critical point of reconnection.

I. INTRODUCTION

Magnetic reconnection is the reordering of magnetic topology, which converts large amounts of magnetic energy into kinetic energy [1–4], thereby powering many of the universe’s most energetic transients. Reconnection likewise governs the interaction between Earth’s magnetosphere and the solar wind [5, 6]. The critical reconnection physics occurs within the electron diffusion region, where the plasma decouples from the magnetic field lines, allowing the lines to snap and reconfigure, and the trigger mechanism for this critical state remains mathematically elusive in magnetohydrodynamic theory.

Our core premise is that magnetic reconnection can be understood as a thermodynamic phase transition. The merits of this position were recently proven by Ref. [7], where the authors demonstrated that, for collisional electrons modelled with kinetic (particle-in-cell) simulations, the reconnection trigger is essentially a temperature threshold, and that the system’s entropy increased dramatically at the transition. In fact, for collisionless reconnection to occur, the electron distribution function must become agyrotropic [4, 8], observations of which have been directly linked to the breakdown of the guiding center approximation [9, 10], caused by the width of the thermal distribution.

In general, the nature of the reconnection trigger is debated, and ‘anomalous’ resistivity, caused by turbulent or stochastic conductivity, is deemed necessary [11]. Such anomalous resistivity has, throughout the space age, been required to account for the fast dissipation rates observed in magnetic reconnection events, empirically described using the Bohm diffusion scaling ($\sim T/B$) [12].

In this article, we derive Bohm resistivity from first principles by treating the magnetized electron fluid as

an overdamped spintronic condensate governed by the Landau-Lifshitz-Gilbert equation [13], representing the breakdown of ideal magnetohydrodynamics. Following renormalization group theory, we posit that at the critical point, the physics of reconnection reduces to the topological constraints of the stable electron gyro-oscillations. To bolster the position, we demonstrate that magnetic reconnection acts as an Adler-Ohmic bifurcation, and the Ohmic response of the system naturally recovers Bohm resistivity. The implication is that the ‘frozen-in’ condition (or guiding center approximation) obeys a tilted washboard potential, mathematically identical to phase locking in Josephson junction theory.

While magnetic topology is traditionally viewed as a non-local constraint, Ref. [14] has recently demonstrated that reconnection rates can be rigorously derived from local field line slippage metrics, validating the notion that the reconnection trigger can be modeled as a local synchronization failure (phase slip). In so doing, we shall defend the position that the ‘anomalous’ resistivity in magnetic reconnection is the macroscopic signature of the electron gyro oscillations failing to maintain coherence against sharp magnetic gradients, thereby spiraling into chaotic orbits.

II. METHODOLOGY

Our goal is to define a minimal model of electron gyro oscillations. For the purposes, we model the electron’s axis of gyration as a rotor that aligns with the local mean field, for which we must define the geometry of alignment on the unit sphere.

We define a lattice of overdamped rotors subject to three competing torques: intrinsic chirality, ferromagnetic exchange, and thermal agitation. The resulting Langevin equation describes the time-evolution of the

* Contact: magnus.fagernes@gmail.com; Also at The European Space Agency Centre for Earth Observation, Frascati, Italy

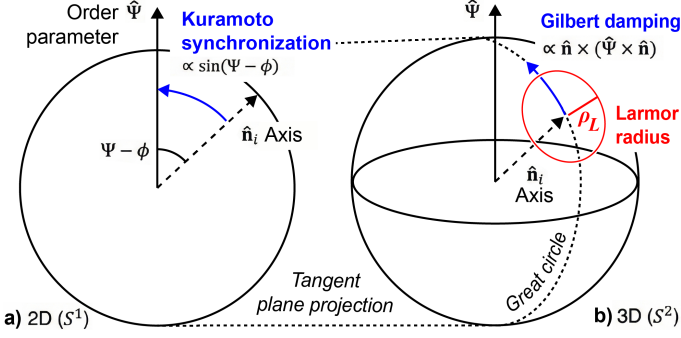


FIG. 1. **Panel a):** the geometry of the two-dimensional tangent plane of the electron gyro rotor, showing how the restoring force acts to align the rotor's axis with the mean field Ψ . **Panel b):** the geometry of the full three-dimensional model, where the electron gyro axis is the unit vector on the unit sphere ($|\hat{n}_i| = 1$), and where the vector torque proportional to $(\hat{n}_i \times \hat{\Psi}) \times \hat{n}_i$ (Eq. 1) acts to align the rotor with the mean field [13].

orientation vector \hat{n}_i [15],

$$\frac{\partial \hat{n}_i}{\partial t} = (\hat{\omega}_i \times \hat{n}_i) + \zeta [\hat{n}_i \times (\hat{\Psi}_i \times \hat{n}_i)] + \eta_i(t). \quad (1)$$

Here, $\hat{\omega}_i$ represents the intrinsic drive (spin precession), $\hat{\Psi}_i$ captures the local alignment field from neighbors, and η_i introduces stochastic (Gaussian) noise fluctuations.

The force interaction is defined by the requirement for rotor i to align with its local neighborhood \mathcal{N}_i , analogous to the Heisenberg ferromagnet [16–18]. The local field $\hat{\Psi}_i$ is the vector sum of neighbors:

$$\hat{\Psi}_i = \sum_{j \in \mathcal{N}_i} \hat{n}_j. \quad (2)$$

Because the rotors are constrained to the unit sphere ($|\hat{n}| = 1$), the alignment torque is the projection of this field onto the rotor's tangent plane, recovering the Landau-Lifshitz torque [13] (see also Ref. [19]),

$$\mathcal{T}_{LL} = \zeta \hat{n}_i \times (\hat{\Psi}_i \times \hat{n}_i). \quad (3)$$

As illustrated in Figure 1, the magnitude of this torque projects to the two-dimensional alignment plane as a Kuramoto-coupling,

$$|\mathcal{T}_{LL}| = \zeta \sin(\Psi_i - \phi_i), \quad (4)$$

establishing that the relevant degree of freedom is the phase mismatch $\delta\phi \equiv \phi_i - \Psi_i$, allowing us to separate the dynamics into an effortless precession around Ψ_i (Goldstone mode) and a dissipative relaxation of the phase mismatch.

The torque \mathcal{T}_{LL} drives the time derivative of the phase mismatch, yielding [20]:

$$\dot{\delta\phi}_i = \omega_i - \zeta \sin(\delta\phi_i), \quad (5)$$

where ω_i is the scalar magnitude of the intrinsic chirality (mismatch). Eq. (5) is recognized as the Adler equation for phase-locking oscillators (Josephson junctions) [21]. This allows us to define the gyro axis slip velocity,

$$v_{\text{slip}} \equiv \langle \dot{\delta\phi} \rangle = \sqrt{\omega_i^2 - \zeta^2}, \quad (6)$$

where a total slippage of π yields field-reversal.

By performing a Taylor expansion of the model's local field around the rotor (see Appendix A), we recover the Landau-Lifshitz-Gilbert equation [13],

$$\frac{\partial \hat{n}_i}{\partial t} = -\omega_i \xi^2 (\hat{n}_i \times \mathbf{H}_{\text{eff}}) - \zeta \xi^2 \hat{n}_i \times (\hat{n}_i \times \mathbf{H}_{\text{eff}}), \quad (7)$$

where chirality is provided by the electron cyclotron frequency Ω_{ce} , via $\omega_i \rightarrow \Omega_{ce} + \delta\omega$, and where the correlation length equals the electron inertial length, $\xi \approx d_e$. By recognizing that $\langle \omega_i \rangle = \Omega_{ce}$, we observe that a broadening of ω_i , which drives the model's dynamics [15, 22, 23]. This is the thermal speed of the electrons $v_{\text{th},i}$, which yields $\omega_i = v_{\text{th},i}/L_{\nabla B}$, $L_{\nabla B}$ being the length-scale of the magnetic gradient [24]. This allows us to define the plasma Adler equation,

$$\dot{\delta\phi}_i = v_{\text{th},i} \left(\frac{1}{L_{\nabla B}} - \frac{1}{\rho_L} \sin(\delta\phi_i) \right), \quad (8)$$

where $\Omega_{ce} = v_{\text{th},i}/\rho_L$, ρ_L being the Larmor radius of the precessing electron [25]. Eq. (8) defines the tilted washboard potential in terms of adiabatic invariance and the breakdown of stable electron orbits [26]. This recovers the magnetohydrodynamic threshold for magnetic reconnection,

$$\rho_L > L_{\nabla B}. \quad (9)$$

This threshold is conventionally derived through considering the magnetic moment μ as no longer conserved (the breakdown of adiabatic invariance), and its recovery from the model, essentially a consideration of vector alignment on the unit sphere, provides justification for the model's application to magnetized plasmas undergoing magnetic reconnection.

As we detail in Appendix A, by quantifying the velocity of the phase-slipping gyro axes, we can describe the work performed by the effective electric field associated with the slippage drift. Ampère's law eventually yields the resistivity,

$$\eta_{\text{spin}}(J) = \eta_0 \sqrt{1 - \left(\frac{J_c}{J} \right)^2} \quad \text{for } J > J_c, \quad (10)$$

where the characteristic resistivity scale is $\eta_0 = \mu_0 \rho_L v_{\text{th},i}$, and where,

$$J_c = \frac{eB^2}{m\mu_0 v_{\text{th},i}} = \frac{B}{\mu_0 \rho_L}, \quad (11)$$

is the critical current, with current $J = |\nabla \times \mathbf{B}|/\mu_0$ being caused by the sharp field gradients. The characteristic resistivity scale simplifies by noting that $\rho_L v_{\text{th},i} \approx k_B T/eB$, meaning that $\eta_0 \propto B^{-1}$. This recovers the Bohm resistivity scaling [27, 28]), a standard phenomenological relation invoked in space & laboratory plasmas [12, 29, 30].

III. RESULTS

We present empirical results from simulations of the two-dimensional tangent plane dynamics, obtained by solving the Adler equation (Eq. 5). This corresponds to the two-dimensional cross-section, the current sheet perpendicular to the magnetic field \mathbf{B} . The spintronic condensate is treated as a discrete lattice of $N \times N$ coupled electron gyro axes, with $N = 512$ (2.6×10^5 rotors), where the state variable is the instantaneous phase of the gyro axis (the rotor) $\phi_{ij} \in [0, 2\pi]$, in the tangent plane projection of the alignment torque (Figure 1), with $\Psi - \phi$ being the polar phase mismatch between the rotor and the local mean field.

From Eq. (5) we observe that the dynamics of the evolving phases are governed by the overdamped Adler equation in the co-rotating Larmor frame (setting $\langle \Omega_{ce} \rangle \equiv 0$), yielding a Kuramoto model [15],

$$\frac{d\phi_i}{dt} = \delta\omega_i(T_e) + KR_i \sin(\Psi_i - \phi_i) + \eta_i(t), \quad (12)$$

where R_i and Ψ_i are the amplitude and phase of the local order parameter, defined by the spatial average over the neighborhood \mathcal{N}_i ,

$$R_i e^{i\Psi_i} = \langle e^{i\phi_j} \rangle_{j \in \mathcal{N}_i}, \quad (13)$$

In our simulations, this average is computed using a Gaussian kernel with width $\sigma = 2.0$ (in units of lattice spacing), representing the exchange interaction length scale $\xi \approx d_e$.

In Eq. (12), K is the coupling constant, and $\delta\omega$ is the temperature-driven “perturbation” to the electron cyclotron frequency, evaluated as a Gaussian random variable with distribution width equal to T_e . We performed $16 \times 16 = 512$ simulations, systematically varying $0.1 < T_e < 3.2$ and $0.032 < K < 10$ in logarithmic increments. This entails varying the ratio $\Gamma = K/T_e$, coupling stiffness divided by noise: $10^{-2} < \Gamma < 10^2$, where transitions are expected around $\Gamma \approx 1$.

From each simulation run, we output two key quantities, (1) topological defect count N_d , equal to the number of nonzero topological winding numbers, q ,

$$q = \frac{1}{2\pi} \oint_C \nabla \phi \cdot d\mathbf{l}, \quad (14)$$

evaluating the entire lattice, and (2) the ensemble average phase slip speed $v_{\text{slip}} = \langle |\dot{\phi} - \dot{\Psi}| \rangle$, the rate at which the electrons’ magnetic moments de-synchronize

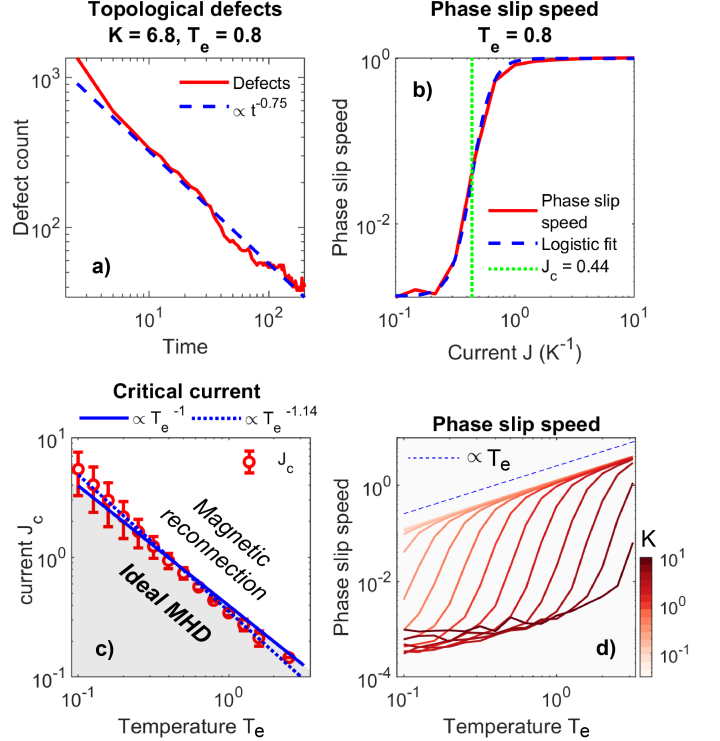


FIG. 2. A statistical aggregate of 512 simulation runs, each featuring a two-dimensional 512×512 lattice, systematically varying $0.1 < T_e < 3.2$ and $0.032 < K < 10$ in logarithmic increments. **Panel a)** shows the defect count (red) and a $t^{-0.75}$ powerlaw fit (blue dashes). **Panel b)** shows the ensemble average phase slip speed (red, evaluated from the second half of 16 simulations with varying values of K), a logistic fit (blue dashes), and J_c , the deflection point in the logistic curve (green dots). **Panel c)** shows J_c for all the simulations, in bins of temperature T_e . Errorbars denote the 95th percent confidence interval of the logistic fit in each bin. Fits of $\propto T_e^{-1.14}$ (determined through non-linear least squares minimization) and $\propto T_e^{-1}$ are shown in blue dashes and blue solid line respectively; the shaded gray region delineates ideal magnetohydrodynamics from magnetic reconnection. **Panel d)** shows ensemble average phase slip speed, varying the temperature (the color of the line indicates the coupling strength K). A $\propto T_e$ fit is shown in blue dashes.

from the magnetic field. An aggregate of these quantities are shown in Figure 2.

Phase synchronization leads to vortices, which merge by synchronizing neighbour rotors. However, Figure 2a) shows that the decay of the defect number density $N_d(t)$ follows a $t^{-0.75}$ scaling [31, 32], markedly slower than the diffusive t^{-1} , and therefore indicative of anomalous transport, consistent with magnetic island coalescence instability in magnetohydrodynamics [33]. Turbulence in our model thereby relaxes via a hierarchical merger of magnetic flux tubes.

Figure 2b) shows the ensemble phase slip speed, for simulations that sweep through coupling K , where we plot against current $J = K^{-1}$, wherein the angular momentum required to decouple the gyro axis from the

mean field ($\omega_i + \eta_i(t)$) is opposed by coupling strength K (Eq. 12), and where we use the magnetohydrodynamic consideration of current as driven by magnetic stress $J = \nabla \times \mathbf{B}/\mu_0$. A logistic fit of v_{slip} against J reveals that the onset of phase slippage is a continuous phase transition with an explosive increase at J_c , the critical current.

Figure 2c) shows the critical current J_c , calculated from 16 logistic plots of 16 ensemble simulations that each sweep through K , sorted by T_e (red circles with errorbars). We observe a near-perfect anti-correlation, with a $\propto T_e^{-1}$ fit adequately describing the data, implying that $J T_e = \text{constant}$. This means that the critical coupling strength required to maintain the phase-locked state scales inversely with the temperature, or, equivalently, the topological lattice breaks when the thermal frustration energy ($k_B T_e$) exceeds the Josephson binding energy of the rotors. The straight line in Figure 2c) thereby delineates ideal magnetohydrodynamics from magnetic reconnection.

Figure 2d) shows 16 curves of v_{slip} against temperature T_e , with a $\propto T_e$ fit shown with blue dashes, showing that when the system enters into phase slippage at the Adler-Ohmic crossover, which happens at hotter temperatures for higher coupling strengths, it does so with an Ohmic scaling.

IV. DISCUSSION

The model simply states that the electron gyro axis, modeled as a rotor in three dimensions, aligns, via a torque, with the mean field. This is the *fundamental microscopic constraint* of ideal magnetohydrodynamics, manifesting the principle of adiabatic invariance [34]. We model the slippage of this alignment, essentially the failure of the first adiabatic invariant during magnetic reconnection.

The foregoing S^2 dynamic in three dimensions then reduces to an S^1 dynamic in two dimensions, by recognizing that the rotor precesses freely, leaving the polar mismatch angle $\delta\phi$ as the effective degree of freedom, and by recognizing that the field-parallel coupling in the reconnection region is strong enough to warrant a two-dimensional lattice in the field-perpendicular plane. This gives us the Adler equation,

$$\dot{\delta\phi}_i = \omega_i - \zeta \sin(\delta\phi_i),$$

and a Kuramoto model in the rotor's tangent plane (Eq. 12). A coupled S^1 oscillator lattice in two dimensions belongs to the XY Universality class [35], or $O(2)$ symmetry group, an assessment that the simulations confirm via the evident hierarchical shock merger (Figure 2a) and the universal scaling of the product $J_c \cdot T_e$ (Figure 2c).

A. Magnetic reconnection as a thermodynamic phase transition

This framework compels a condensed matter perspective. The specific microscopic interaction details (such as exact particle trajectories governed by Lorentz forces) become irrelevant operators under renormalization flow [36], owing to a set of shared critical exponents at the critical point [37]. Consequently, the topology is agnostic to the specific interaction length d_e , which serves here merely as the necessary dimensional calibration for the universal geometry. The logistic breakdown of the “frozen-in” condition is therefore identified as the universal signature of the Berezinskii-Kosterlitz-Thouless (BKT) transition [35, 38], in which framework the ‘critical current’ J_c represents the unbinding threshold for topological vortex pairs. Magnetic reconnection is thus identified as a thermodynamic phase transition.

The foregoing is supported in the recent literature. Kinetic simulations by Ref. [7] have confirmed that the onset of collisionless reconnection exhibits the signature of a thermodynamic phase transition, characterized by a discontinuity in the current sheet's heat capacity. Our spintronic framework provides the topological mechanism explaining Ref. [7]’s result: the ‘disordered phase’ corresponds to the Adler-Ohmic slippage regime where gyrophase coherence is irreducibly lost.

Application of renormalization group theory leads directly to our treatment of magnetic reconnection as phase slippage in an overdamped spintronic condensate. That we recover the conventional magnetohydrodynamic reconnection trigger (Eq. 9), magnetic island coalescence (Figure 2a), curvature drift (Eq. 31), and Bohm resistivity (Eq. 10), empirically validates the description.

B. Bohm resistivity

The onset of magnetic reconnection in our overdamped spintronic condensate with increasing current J (steepening magnetic field gradients), is shown in Figure 2b) to be extremely sharp, modeled with a logistic function, consistent with observations of fast, “bursty”, even transient magnetic reconnection [39–42]. Since the slipping rotors cause electrons to take on chaotic and dissipative orbits, this recognition constitutes a first-principles theoretical prediction and empirical verification of anomalous, or Bohm, resistivity ($\eta \propto T/B$), a long-time empirical assumption for space plasmas [28, 43, 44], whose onset as a topological phase transition here emerges naturally: the resistivity is proportional to the phase slip velocity, which saturates at the electron thermal speed T_e . The phase transition we observe is explosive, which matches the observed sudden release dynamics observed in solar flares [11, 45].

The reliance on the BKT transition provides an explanation for the curious 1/16 factor usually seen in the Bohm diffusion coefficient [28].

The recovery of Bohm resistivity is a significant result. For some 70 years, the discrepancy between observed and theorized plasma diffusion rates, termed *anomalous* diffusion, has been phenomenologically patched using Bohm resistivity [12, 28, 43, 44, 46–49]. The overdamped spintronic condensate model of a magnetized plasma predicts that the onset of Bohm-like resistivity is an Adler-Ohmic bifurcation, suggesting that Bohm resistivity may be directly caused by electron gyrophase slippage, events that are already necessitated by the breakdown of the guiding center approximation [9, 10]. The natural consequence is that Bohm resistivity is a topological property of magnetized matter rather than a turbulent effect, arising at critical points such as magnetic reconnection, when the system effectively ignores microscopic restraints and yields to universal topological constraints.

C. The overdamped spintronic condensate

Our findings are contingent on the careful mapping of electron gyro axes in a magnetized plasma to a 3D lattice of rotors aligned with the mean field via a Gilbert damping torque (Figure 1), essentially a *classical, overdamped spintronic condensate*. Since this topological lattice is inherently scale-invariant, the correlation length ξ is identified with the electron inertial length d_e rather than derived, to physically anchor the universality class. While the geometric mapping is demonstrably accurate, the overdamped condition deserves scrutiny.

Theoretically, it implies that the timescale of magnetic relaxation ($1/\Omega_{ce}$) is much shorter than the driving timescale (the shearing rate of the magnetic field). In terms of microphysics, this corresponds to a regime where electrons are subject to current-driven micro-instabilities (e.g., Buneman or Ion-Acoustic modes), triggered when the drift velocity exceeds a critical acoustic threshold ($v_d > C_s$) [50]. As detailed in Ref. [51], increasing drift beyond this threshold generates intense turbulence, scattering and heating the electrons. This anomalous heating raises the stability threshold, creating a feedback loop where the drift is effectively clamped by the growing thermal pressure. Consequently, in the limit of strong driving, the system behaves as if governed by a drag force scaling with the thermal speed v_{th} . In this turbulent marginal stability regime, anomalous drag vastly exceeds the inertial term, rendering the electrons effectively *overdamped*.

This reduces the second-order Newtonian equation of motion for the rotors to the first-order Adler equation [52] (see Eqs. 5, 26), effectively filtering out high-frequency cyclotron resonances to isolate the slow-manifold topological dynamics [53]. Here, the inertia suppressed by the overdamped approximation is replaced by a thermodynamic closure, where work is dissipated directly into the thermal pool.

A posteriori support for this notion comes from considering that the overdamped condition directly leads to

a slippage electric field \mathbf{E}_{eff} that scales identically to the current tension electric field \mathbf{E}_{CT} (Eq. 43) [54], caused by electron inertia.

Although the overdamped condition physically suppresses electron inertia, the fact that the resulting gyro axis slip field mirrors the inertial current tension field, as well as the recovery of the ideal magnetohydrodynamic breakdown threshold (Eq. 9), implies that phase stiffness is a topological equivalence for electron inertia (see, e.g., Refs. [15, 22]). Our model thereby successfully isolates the universal energetic barrier for reconnection, treating the kinetic resistance to turning as a mathematically equivalent thermodynamic potential.

D. Whistler magnons

Lastly, by explicitly mapping the spintronic condensate to electron gyro axes ($\xi \rightarrow d_e$ and $\omega_i \rightarrow \Omega_{ce} + \delta\omega_i$, see Appendix A), we recover in the condensate the presence of *ferromagnetic magnons* (see, e.g., Ref. [55] for a review). These are spin waves that ripple through the precessing, slipping electron gyro axes, which advect enstrophy. The dispersion relation reads (see the Appendices),

$$\omega(k) = \Omega_{ce} d_e^2 k^2 - i\zeta d_e^2 k^2, \quad (15)$$

which is the exact dispersion relation for whistler-mode plasma waves [29, 30]. Since the gyro axes and the magnetic topology are mutually dependent, this results indicates that, in the phase slipping regime, magnons propagate through the precessing gyro axes in tandem with whistler waves, the latter of which then obtain a *topological footprint*. ζ in Eq. (40) is given by the Landau-Lifshitz torque (Gilbert damping). In a collisionless plasma, this energy loss corresponds to Landau damping or wave-particle resonance extracting energy from the topological rearrangement. Our model is scale-invariant, and so the mean-field coupling ζ can be predicted in observations of whistler wave-particle interactions. The whistler magnons should therefore capture the conventional whistler-mode energy transport with an equivalent transport of *enstrophy*.

V. CONCLUSION

We have formulated the Landau-Lifshitz-Gilbert equation for an overdamped spintronic condensate, and demonstrate that this model makes unique predictions for magnetic reconnection, namely the onset of anomalous resistivity. This justifies the application of renormalized group theory, which, in turn, indicates that magnetic reconnection can be understood as a topological phase transition of the *XY* universality class [35]. We provide empirical evidence that the onset of electron gyrophase slippage follows universal BKT scaling laws [38], which yield a non-linear anomalous resistivity that rigorously

recovers the empirical Bohm scaling. We thereby provide a first-principles origin for anomalous diffusion in space plasmas.

Our results are consistent with renormalization flow governing the breakdown of magnetohydrodynamics, anchoring magnetic reconnection to the same fundamental dynamics that govern ferromagnetism: the Landau-Lifshitz-Gilbert equation [13]. While the microphysics differ, the macroscopic physics of all such systems converge at critical points to the topological constraints dictated by the relaxation of a vector order parameter in a symmetry-breaking field.

ACKNOWLEDGEMENTS

This work is supported by the European Space Agency's Living Planet Grant No. 1000012348. The author is grateful to O. Nestande, D. Knudsen, PT. Jayachandran, and K. Douch for stimulating discussions. Google's Gemini 3.0 Pro has been used for mathematical formalism and coding assistance in MATLAB.

APPENDIX A: THEORETICAL FOUNDATION

Following Ref. [15], we start with the Adler equation (Eq. 5). We calculate the time required for a complete 2π phase slip:

$$T_{\text{slip}} = \int_0^{2\pi} \frac{d\delta\phi}{\dot{\delta\phi}} = \int_0^{2\pi} \frac{d\delta\phi}{\omega_i - \zeta \sin(\delta\phi)} = \frac{2\pi}{\sqrt{\omega_i^2 - \zeta^2}}, \quad (16)$$

where we assumed the running state ($\omega_i > \zeta$). Consequently, the slip velocity is defined as the inverse of the slip period:

$$v_{\text{slip}} \equiv \langle \dot{\phi} \rangle = \frac{2\pi}{T_{\text{slip}}} = \sqrt{\omega_i^2 - \zeta^2}, \quad (17)$$

where we note that v_{slip} is a time-averaged quantity (over slip cycles), and where we stress that this is the slippage of the phase of the *gyro axis*, not the electron's gyrophase, and that the latter slips when the former does so. Magnetic field-reversal follows from the gyro axis slipping π .

A. The Landau-Lifshitz-Gilbert equation

Examining the hydrodynamic limit, we must assume that intrinsic chirality is aligned with the mean field, $\hat{\omega}_i \approx \omega_i \hat{\Psi}$. We can then write Eq. (1) as,

$$\frac{\partial \hat{n}}{\partial t} \approx \omega_i (\hat{\Psi} \times \hat{n}) + \zeta [\hat{n} \times (\hat{\Psi} \times \hat{n})]. \quad (18)$$

Next, we perform a Taylor expansion of the local field around the chiral rotor. This introduces the Laplacian, transforming the discrete lattice into a continuous

medium [15],

$$\hat{\Psi}(\mathbf{r}, t) \approx \rho (\hat{n} + \xi^2 \nabla^2 \hat{n}), \quad (19)$$

where ξ is the correlation length (interaction radius), and $\nabla^2 \hat{n}$ is the curvature of the field. We substitute Eq. (19) into Eq. (18),

$$\frac{\partial \hat{n}}{\partial t} \approx -\omega_i \xi^2 (\hat{n} \times \nabla^2 \hat{n}) + \zeta \xi^2 [\hat{n} \times (\hat{n} \times \nabla^2 \hat{n})]. \quad (20)$$

Setting $\mathbf{H}_{\text{eff}} = \nabla^2 \hat{n}$, we recover the Landau-Lifshitz-Gilbert equation in standard form [13],

$$\frac{\partial \hat{n}}{\partial t} = -\frac{\gamma}{1 + \alpha^2} (\hat{n} \times \mathbf{H}_{\text{eff}}) - \frac{\gamma \alpha}{1 + \alpha^2} \hat{n} \times (\hat{n} \times \mathbf{H}_{\text{eff}}). \quad (21)$$

Matching the terms yields the constitutive relations,

$$\alpha = \frac{\zeta}{\omega_i}, \quad (22)$$

and

$$\gamma = \omega_i \xi^2 (1 + \alpha^2), \quad (23)$$

allowing us to write the Landau-Lifshitz-Gilbert equation on the form,

$$\frac{\partial \hat{n}_i}{\partial t} = -\omega_i \xi^2 (\hat{n}_i \times \mathbf{H}_{\text{eff}}) - \zeta \xi^2 \hat{n}_i \times (\hat{n}_i \times \mathbf{H}_{\text{eff}}). \quad (24)$$

In the next section, we shall use this model to rigorously describe the phase mismatch between the electron gyro axis and the local mean field in a magnetized plasma.

B. Gyrophase slippage & spintronic reconnection

Consider the angular motion of the electron gyro axis itself as a source of *chirality*, or frustration, ω_i , a distribution that obeys $\langle \omega_i \rangle = \Omega_{ce}$, the electron cyclotron frequency. Then, an increase in the spread of ω_i , which correspond to thermal broadening and relativistic mass correction, will proportionally increase the sum total enstrophy, eventually reaching the point when the magnetic topology can no longer support the guiding centre approximation, at which point magnetic reconnection will have occurred. The trigger is an Adler-Ohmic crossover (Eq. 5), and after this, continuous gyrophase slippage causes an irreversible reduction in energy, by inducing chaotic electron orbits [56].

To implement the foregoing, we apply the minimal model that was defined in the previous section. The vector \hat{n}_i becomes the electron's magnetic moment $\mathbf{\mu}_i$ aligning against \mathbf{B} , but whose axis of precession in general takes the form \hat{n}_i . The force that seeks to stabilize the orbit is the dissipative Landau-Lifshitz torque, which acts to align the electron's gyration axis with the local magnetic field [57]. This alignment torque takes the Gilbert form:

$$\mathcal{T}_{\text{LL}} = \zeta \hat{n}_i \times (\mathbf{b}_i \times \hat{n}_i), \quad (25)$$

where $\mathbf{b} = \mathbf{B}/B$ is the unit magnetic field vector. When \hat{n}_i and \mathbf{b} aligns, the electron gyro axis is perfectly ‘‘frozen-in,’’ and, as we shall demonstrate, *trapped*. The mismatch between the two, $\delta\phi$, therefore measures whether the electron is orbiting a magnetic field-line in a stable manner or entering a chaotic orbit [56].

We can now write the plasma Adler equation,

$$\dot{\delta\phi} = v_{\text{th},i} \left(\frac{1}{L_{\nabla B}} - \frac{1}{\rho_L} \sin(\delta\phi) \right), \quad (26)$$

where $\Omega_{ce} = v_{\text{th},i}/\rho_L$ is the electron cyclotron frequency, ρ_L being the Larmor radius of the precessing electron [25], and where we replace chirality ω_i with the rate at which the magnetic field direction changes, $v_{\text{th},i}/L_{\nabla B}$, where $L_{\nabla B}$ is the length-scale of the magnetic gradient and $v_{\text{th},i}$ is the (thermal) speed of the electron [24].

Eq. (26) expresses that electrons are ‘‘running’’ when they can no longer sustain perfect orbits around a field line, crossing the limit of adiabatic invariance [26]. Here, we recover the magnetohydrodynamic threshold for magnetic reconnection,

$$\rho_L > L_{\nabla B}. \quad (27)$$

This threshold is conventionally derived through considering the magnetic moment μ as no longer conserved (the breakdown of adiabatic invariance). In the present article, we have derived the same result purely from a consideration of vector alignment on the unit sphere.

Next, we shall demonstrate that the inherently nonlinear and explosive nature of the Adler slip velocity (Eq. 17) fuels the anomalous resistivity that accompanies magnetic reconnection.

C. Magnetic reconnection & anomalous resistivity

To quantify the anomalous resistivity, we decompose the electron drift velocity,

$$\mathbf{v}_{\text{total}} = \mathbf{v}_{\text{ideal}} + \mathbf{v}_{\text{slip}}, \quad (28)$$

where $\mathbf{v}_{\text{ideal}} = (\mathbf{E} \times \mathbf{B})/B^2$ is the ideal, frozen-in drift. The deviation from this ideal state is the spintronic slip velocity, whose magnitude is governed by the Adler-Ohmic bifurcation derived in Sec. :

$$|\mathbf{v}_{\text{slip}}| = \rho_L \sqrt{\frac{v_{\text{th},i}^2}{L_{\nabla B}^2} - \Omega_{ce}^2}, \quad (29)$$

where we multiplied the angular slip velocity (Eq. 17) with the Larmor radius ρ_L . This slip motion generates an anomalous motional electric field (resistivity),

$$\mathbf{E}_{\text{eff}} = -\mathbf{v}_{\text{slip}} \times \mathbf{B}, \quad (30)$$

which breaks the frozen-flux condition whenever $\rho_L > L_{\nabla B}$. In the running state ($\omega_i \gg \zeta$), we can write,

$$|\mathbf{v}_{\text{slip}}| \approx \frac{v_{\text{th},i}\rho_L}{L_{\nabla B}}, \quad (31)$$

where we observe that the magnitude of the cross-field slippage scales identically to the standard curvature drift [58], yet represents a diffusive flux perpendicular to the magnetic field. The magnitude of Eq. (30) is given by,

$$E_{\text{eff}} = |\mathbf{v}_{\text{slip}}|B, \quad (32)$$

and after inserting the non-linear Adler slip velocity, we obtain,

$$E_{\text{eff}} \approx B \left(\rho_L \sqrt{\left(\frac{v_{\text{th},i}}{L_{\nabla B}} \right)^2 - \Omega_{ce}^2} \right). \quad (33)$$

To find the resistivity η , we must express the field gradient scale $L_{\nabla B}$ in terms of the current density J , which, using Ampère’s law ($\nabla \times \mathbf{B} = \mu_0 \mathbf{J}$, μ_0 being magnetic permittivity), leads to the following approximation,

$$\frac{1}{L_{\nabla B}} \approx \frac{|\nabla B|}{B} \approx \frac{\mu_0 J}{B}, \quad (34)$$

which we can readily substitute into Eq. (33),

$$E_{\text{eff}} \approx B \rho_L \sqrt{\left(v_{\text{th},i} \frac{\mu_0 J}{B} \right)^2 - \Omega_{ce}^2}. \quad (35)$$

From this, and Eq. (27), we observe the threshold spintronic critical current J_c :

$$v_{\text{th},i} \frac{\mu_0 J_c}{B} = \Omega_{ce} \implies J_c = \frac{eB^2}{m\mu_0 v_{\text{th},i}}, \quad (36)$$

or,

$$J_c = \frac{B}{\mu_0 \rho_L}, \quad (37)$$

which corresponds to the current density where the electron Larmor radius equals the current sheet width, $\rho_L = L$).

To transform this into the standard Ohmic form $E = \eta J$, we factor out the drive coefficient $(v_{\text{th},i}\mu_0/B)^2$ from the square root. This cancels the magnetic field B , leaving the current J as the primary variable,

$$E_{\text{eff}} \approx (\mu_0 \rho_L v_{\text{th},i}) J \sqrt{1 - \left(\frac{J_c}{J} \right)^2}, \quad (38)$$

revealing the spintronic anomalous resistivity as the coefficient,

$$\eta_{\text{spin}}(J) = \eta_0 \sqrt{1 - \left(\frac{J_c}{J} \right)^2} \quad \text{for } J > J_c. \quad (39)$$

Here, we make two observations:

(1) the characteristic resistivity scale is $\eta_0 = \mu_0 \rho_L v_{\text{th},i}$, which, since $\rho_L v_{\text{th},i} \approx k_B T/eB$, means that we recover the Bohm resistivity scaling [27, 28]), a standard phenomenological assumption in space plasmas [29, 30].

(2) the spintronic critical current provides a hard trigger, $\sqrt{1 - (J_c/J)^2}$, below which the anomalous resistivity is strictly zero (ideal magnetohydrodynamics). when the current density J exceeds the critical threshold J_c (the Adler limit), the electrons cascade non-linearly into a resistive state, triggering magnetic reconnection.

D. Spin waves

The precession of the gyro axis around the mean field, which is, under the guiding centre approximation, assumed to be effectively averaged out, can in fact drive a Goldstone mode, manifesting as ferromagnetic magnons, or spin waves, that propagate through the phase-slipping rotors. We can derive the dispersion relation from Eq. (24), which yields (see Appendix B),

$$\omega(k) = \frac{\gamma k^2}{1 + \alpha^2} - i \frac{\gamma \alpha k^2}{1 + \alpha^2}, \quad (40)$$

where the real part corresponds to the magnon and the imaginary part as its decay.

We now apply the specific plasma parameters:

(1) $\omega_i \approx \Omega_{ce}$, which equates chirality with the electron cyclotron frequency, while recognizing that it should strictly read $\omega_i \rightarrow \Omega_{ce} + \delta\omega$, where $\delta\omega$ averages out.

(2) $\xi \approx d_e$ (setting the correlation length approximately equal to the electron inertial length).

The final derived coefficient for the spintronic stiffness is,

$$\gamma = \Omega_{ce} d_e^2 (1 + \alpha^2), \quad (41)$$

allowing us to write the dispersion relation as,

$$\omega(k) = \Omega_{ce} d_e^2 k^2 - i \zeta d_e^2 k^2. \quad (42)$$

To see the significance of this result, consider the following. A magnon ripples through the phase-slipping rotors. The rotors, in turn, being electron gyro axes, drag the magnetic topology \hat{b} , meaning that the magnons should be visible in electric and magnetic fields measured *in-situ*. This is because the magnons experience friction (α in Eq. 24), by which the spin wave's coherence is thermalized to the dissipative bath. Eq. (42) describes the dispersion relation for whistler-mode plasma waves, which are excited in the same region, after which they propagate outward, damping their energy into the electrons and thereby heating them [30, 59]. The ferromagnetic magnons that propagate through the slipping gyro rotors in the spintronic condensate are therefore the topological footprint of whistler waves.

E. Verification

The foregoing effective electric field \mathbf{E}_{eff} is consistent with recent research that considered the effects of the

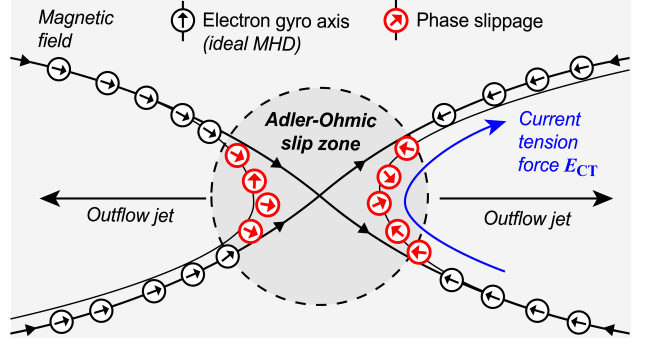


FIG. 3. Illustration of a reconnection event in the overdamped spintronic condensate (black and red compasses representing rotors that align with the magnetic field). The current tension electric field is indicated, which causes slipping electrons to enter the outflow jets.

current tension electric field [54],

$$\mathbf{E}_{CT} = -\frac{m}{e} \left[\left(\frac{\mathbf{J}}{en} \cdot \nabla \right) \frac{\mathbf{J}}{en} \right], \quad (43)$$

that is, the electron inertia associated with the spatial variation of the current flow. E_{CT} is often ignored as a small number, but proven consequential inside the electron diffusion region [54], contributing to the reconnection electric field. In our framework, E_{CT} appears when the current tension can no longer sustain electron gyrations, causing the resistive drifts (Eq. 39). In Figure 3 we illustrate this term (in blue), along with the reconnection X-line, with aligned gyro axes in black compasses, and gyrophase slipping electrons in red compasses.

It is crucial to distinguish the physical nature of the spintronic slip velocity, \mathbf{v}_{slip} , from the standard guiding center drifts of ideal magnetohydrodynamics. While the magnitude of the slip velocity in the running state, $|\mathbf{v}_{\text{slip}}| \approx v_{\text{th},i} \rho L / L_{\nabla B}$, algebraically recovers the scaling of standard curvature drift, the two represent topologically distinct regimes of motion. Standard curvature drift is an adiabatic process: the electron's gyrophase orbit remains closed and the first adiabatic invariant (magnetic moment μ) is conserved. In contrast, the Adler-Ohmic slip represents a dissipative failure of this orbit closure. When the drive exceeds the lock ($\omega_i > \zeta$), the electron crosses the limit of adiabatic invariance, and the gyration effectively 'opens' into a chaotic spiral. Unlike adiabatic drift, which is reversible performs no work, this phase slippage generates entropy, manifesting macroscopically as the anomalous resistive field \mathbf{E}_{eff} that breaks the frozen-in topology.

APPENDIX B: THE DISPERSION RELATION

We begin with the Landau-Lifshitz-Gilbert equation on the form,

$$\frac{\partial \hat{n}}{\partial t} = -\gamma \hat{n} \times H_{\text{eff}} + \alpha \hat{n} \times \frac{\partial \hat{n}}{\partial t} \quad (44)$$

We consider the polarized case, and introduce a small transverse perturbation \vec{m} (the magnon),

$$\hat{n}(\vec{r}, t) \approx \hat{z} + \vec{m}(\vec{r}, t), \quad (45)$$

where $\vec{m} = (m_x, m_y, 0)$ and $|\vec{m}| \ll 1$. We substitute this into the effective field definition $H_{\text{eff}} \approx \nabla^2 \vec{m}$, and then substitute this into Eq. (44), keeping only linear terms,

$$\frac{\partial \vec{m}}{\partial t} = -\gamma(\hat{z} \times \nabla^2 \vec{m}) + \alpha(\hat{z} \times \frac{\partial \vec{m}}{\partial t}). \quad (46)$$

We solve this for the eigenmodes by assuming a plane wave solution with frequency ω and wavenumber k :

$$\vec{m}(\vec{r}, t) = \vec{m}_0 e^{i(\vec{k} \cdot \vec{r} - \omega t)}. \quad (47)$$

Operators transform as $\partial/\partial t \rightarrow -i\omega$ and $\nabla^2 \rightarrow -k^2$, which yields,

$$-i\omega \vec{m} = -\gamma[\hat{z} \times (-k^2 \vec{m})] + \alpha[\hat{z} \times (-i\omega \vec{m})]. \quad (48)$$

We simplify the cross products (since \hat{z} points upwards),

$$-i\omega \vec{m} = \gamma k^2(\hat{z} \times \vec{m}) - i\alpha\omega(\hat{z} \times \vec{m}), \quad (49)$$

or,

$$-i\omega \vec{m} = (\gamma k^2 - i\alpha\omega)(\hat{z} \times \vec{m}). \quad (50)$$

To solve for ω , we apply the circular polarization ansatz naturally favored by chiral systems: Let $m_+ = m_x + im_y$. The cross product operation $\hat{z} \times \vec{m}$ corresponds to multiplication by $-i$:

$$(\hat{z} \times \vec{m})_+ = -im_+. \quad (51)$$

Substituting this scalar equivalent into the vector equation:

$$-i\omega m_+ = (-i\gamma k^2 - \alpha\omega)m_+, \quad (52)$$

which, after dividing by the amplitude m_+ (assuming non-zero perturbation), yields,

$$-i\omega = -i\gamma k^2 - \alpha\omega. \quad (53)$$

We rearrange this to isolate ω ,

$$\omega = \frac{i\gamma k^2}{i - \alpha} = \frac{\gamma k^2(1 - i\alpha)}{1 + \alpha^2}. \quad (54)$$

This yields the dispersion relation for the phase slippage magnons,

$$\omega(k) = \frac{\gamma k^2}{1 + \alpha^2} - i \frac{\gamma \alpha k^2}{1 + \alpha^2}. \quad (55)$$

[1] S. W. H. Cowley, TUTORIAL: Magnetosphere-Ionosphere Interactions: A Tutorial Review, Washington DC American Geophysical Union Geophysical Monograph Series **118**, 91 (2000).

[2] R. M. Kulsrud, Magnetic reconnection: Sweet-Parker versus Petschek, Earth, Planets and Space **53**, 417 (2001).

[3] S. E. Milan, G. Provan, and B. Hubert, Magnetic flux transport in the Dungey cycle: A survey of dayside and nightside reconnection rates, Journal of Geophysical Research: Space Physics **112**, 10.1029/2006JA011642 (2007).

[4] J. Egedal, W. Daughton, and A. Le, Large-scale electron acceleration by parallel electric fields during magnetic reconnection, Nature Physics **8**, 321 (2012).

[5] R. Fujii and T. Iijima, Control of the ionospheric conductivities on large-scale Birkeland current intensities under geomagnetic quiet conditions, Journal of Geophysical Research: Space Physics **92**, 4505 (1987).

[6] R. Bruno and V. Carbone, The Solar Wind as a Turbulence Laboratory, Living Reviews in Solar Physics **10**, 2 (2013).

[7] J. Jara-Almone and H. Ji, Thermodynamic Phase Transition in Magnetic Reconnection, Physical Review Letters **127**, 055102 (2021).

[8] M. Hesse, K. Schindler, J. Birn, and M. Kuznetsova, The diffusion region in collisionless magnetic reconnection, Physics of Plasmas **6**, 1781 (1999).

[9] J. D. Scudder, F. S. Mozer, N. C. Maynard, and C. T. Russell, Fingerprints of collisionless reconnection at the separator, I, Ambipolar-Hall signatures, Journal of Geophysical Research: Space Physics **107**, SMP 13 (2002).

[10] J. D. Scudder, H. Karimabadi, W. Daughton, and V. Roytershteyn, Frozen flux violation, electron demagnetization and magnetic reconnection, Physics of Plasmas **22**, 101204 (2015).

[11] S. Tsuneta, Structure and dynamics of magnetic reconnection in a solar flare, The Astrophysical Journal **456**, 840 (1996).

[12] H. R. Kaufman, Explanation of Bohm diffusion, Journal of Vacuum Science & Technology B: Microelectronics Processing and Phenomena **8**, 107 (1990).

[13] M. Lakshmanan, The fascinating world of the Landau-Lifshitz-Gilbert equation: An overview, Philosophical Transactions of the Royal Society A: Mathematical, Physical and Engineering Sciences **369**, 1280 (2011).

[14] D. MacTaggart, On Field Line Slippage Rates in the Solar Corona, *Solar Physics* **300**, 48 (2025).

[15] M. F. Ivarsen, Information supercurrents and spin waves in chiral active matter: Universality of the Landau-Lifshitz-Gilbert equation (2025), arXiv:2512.16884 [cond-mat].

[16] T. Vicsek, A. Czirók, E. Ben-Jacob, I. Cohen, and O. Shochet, Novel Type of Phase Transition in a System of Self-Driven Particles, *Physical Review Letters* **75**, 1226 (1995).

[17] J. Toner and Y. Tu, Flocks, herds, and schools: A quantitative theory of flocking, *Physical Review E* **58**, 4828 (1998).

[18] M. C. Marchetti, J. F. Joanny, S. Ramaswamy, T. B. Liverpool, J. Prost, M. Rao, and R. A. Simha, Hydrodynamics of soft active matter, *Reviews of Modern Physics* **85**, 1143 (2013).

[19] M. A. Lohe, Non-Abelian Kuramoto models and synchronization, *Journal of Physics A: Mathematical and Theoretical* **42**, 395101 (2009).

[20] S. H. Strogatz, R. E. Mirollo, and P. C. Matthews, Coupled nonlinear oscillators below the synchronization threshold: Relaxation by generalized Landau damping, *Physical Review Letters* **68**, 2730 (1992).

[21] L. Danner, C. Padurariu, J. Ankerhold, and B. Kubala, Injection locking and synchronization in Josephson photonics devices, *Physical Review B* **104**, 054517 (2021).

[22] M. F. Ivarsen, Onsager Condensation in Chiral Active Matter: Universality of Supersonic Topological Gas Dynamics (2025), arXiv:2512.01884 [cond-mat].

[23] M. F. Ivarsen, Kinetic Turing Instability and Emergent Spectral Scaling in Chiral Active Turbulence (2025), arXiv:2508.21012 [physics].

[24] Introduction, in *Basic Space Plasma Physics* (WORLD SCIENTIFIC, 2022) pp. 1–14, 3rd ed.

[25] K. Stasiewicz, Finite Larmor radius effects in the magnetosphere, *Space Science Reviews* **65**, 221 (1993).

[26] J. Büchner and L. M. Zelenyi, Regular and chaotic charged particle motion in magnetotaillike field reversals: 1. Basic theory of trapped motion, *Journal of Geophysical Research: Space Physics* **94**, 11821 (1989).

[27] S. I. Braginskii, Transport Processes in a Plasma, *Reviews of Plasma Physics* **1**, 205 (1965).

[28] T. Ott and M. Bonitz, Diffusion in a Strongly Coupled Magnetized Plasma, *Physical Review Letters* **107**, 135003 (2011).

[29] R. A. Treumann and W. Baumjohann, *Advanced Space Plasma Physics*, Vol. 30 (Imperial College Press London, 1997).

[30] J. L. Burch, R. B. Torbert, T. D. Phan, L.-J. Chen, T. E. Moore, R. E. Ergun, J. P. Eastwood, D. J. Gershman, P. A. Cassak, M. R. Argall, S. Wang, M. Hesse, C. J. Pollock, B. L. Giles, R. Nakamura, B. H. Mauk, S. A. Fuselier, C. T. Russell, R. J. Strangeway, J. F. Drake, M. A. Shay, Yu. V. Khotyaintsev, P.-A. Lindqvist, G. Marklund, F. D. Wilder, D. T. Young, K. Torkar, J. Goldstein, J. C. Dorelli, L. A. Avanov, M. Oka, D. N. Baker, A. N. Jaynes, K. A. Goodrich, I. J. Cohen, D. L. Turner, J. F. Fennell, J. B. Blake, J. Clemmons, M. Goldman, D. Newman, S. M. Petrinec, K. J. Trattner, B. Lavraud, P. H. Reiff, W. Baumjohann, W. Magnes, M. Steller, W. Lewis, Y. Saito, V. Coffey, and M. Chandler, Electron-scale measurements of magnetic reconnection in space, *Science* **352**, aaf2939 (2016).

[31] G. F. Carnevale, J. C. McWilliams, Y. Pomeau, J. B. Weiss, and W. R. Young, Evolution of vortex statistics in two-dimensional turbulence, *Physical Review Letters* **66**, 2735 (1991).

[32] V. D. Larichev and J. C. McWilliams, Weakly decaying turbulence in an equivalent-barotropic fluid, *Physics of Fluids A: Fluid Dynamics* **3**, 938 (1991).

[33] J. C. Dorelli and J. Birn, Electron magnetohydrodynamic simulations of magnetic island coalescence, *Physics of Plasmas* **8**, 4010 (2001).

[34] T. G. Cowling, *Magnetohydrodynamics* (Interscience Publishers, 1957).

[35] J. M. Kosterlitz and D. J. Thouless, Ordering, metastability and phase transitions in two-dimensional systems, *Journal of Physics C: Solid State Physics* **6**, 1181 (1973).

[36] K. G. Wilson, Renormalization Group and Critical Phenomena. I. Renormalization Group and the Kadanoff Scaling Picture, *Physical Review B* **4**, 3174 (1971).

[37] M. E. Fisher, The renormalization group in the theory of critical behavior, *Reviews of Modern Physics* **46**, 597 (1974).

[38] V. Berezinskii, Destruction of long-range order in one-dimensional and two-dimensional systems having a continuous symmetry group I. Classical systems, *Sov. Phys. JETP* **32**, 493 (1971).

[39] H. U. Frey, D. Han, R. Kataoka, M. R. Lessard, S. E. Milan, Y. Nishimura, R. J. Strangeway, and Y. Zou, Dayside Aurora, *Space Science Reviews* **215**, 51 (2019).

[40] D. J. Southwood, C. J. Farrugia, and M. A. Saunders, What are flux transfer events?, *Planetary and Space Science* **36**, 503 (1988).

[41] K. Oksavik, J. Moen, and H. C. Carlson, High-resolution observations of the small-scale flow pattern associated with a poleward moving auroral form in the cusp, *Geophysical Research Letters* **31**, 10.1029/2004GL019838 (2004).

[42] M. F. Ivarsen, J.-P. St-Maurice, G. C. Hussey, K. McWilliams, Y. Jin, D. R. Huyghebaert, Y. Miyashita, and D. Sibeck, Eastward transients in the dayside ionosphere. II. A parallel-plate capacitor-like effect, *Physical Review E* **112**, 045203 (2025).

[43] H. Okuda, J. M. Dawson, and W. M. Hooke, Interpretation of an Enhanced Diffusion Observed in a Solid-State Plasma, *Physical Review Letters* **29**, 1658 (1972).

[44] D. D. Millar, Ion currents, ion-neutral collisions and plasma transport phenomena, *Australian Journal of Physics* **29**, 249 (1976).

[45] J. Heyvaerts, E. R. Priest, and D. M. Rust, An emerging flux model for the solar flare phenomenon, *The Astrophysical Journal* **216**, 123 (1977).

[46] R. W. Hockney, Computer Experiment of Anomalous Diffusion, *The Physics of Fluids* **9**, 1826 (1966).

[47] H. Okuda and J. M. Dawson, Theory and numerical simulation on plasma diffusion across a magnetic field, *The Physics of Fluids* **16**, 408 (1973).

[48] M. C. Marchetti, T. R. Kirkpatrick, and J. R. Dorfman, Anomalous diffusion of charged particles in a strong magnetic field, *Physical Review A* **29**, 2960 (1984).

[49] D. Curreli and F. F. Chen, Cross-field diffusion in low-temperature plasma discharges of finite length, *Plasma Sources Science and Technology* **23**, 064001 (2014).

[50] O. Buneman, Excitation of Field Aligned Sound Waves by Electron Streams, *Physical Review Letters* **10**, 285 (1963).

[51] J.-P. St.-Maurice and J. L. Chau, A theoretical framework for the changing spectral properties of meter-scale Farley-Buneman waves between 90 and 125 km altitudes, *Journal of Geophysical Research: Space Physics* **121**, 10,341 (2016).

[52] M. Tinkham, *Introduction to Superconductivity* (Courier Corporation, 2004).

[53] J. Carr, *Applications of Centre Manifold Theory*, Applied Math. Sci. Vol. 35, Vol. 35 (Springer-Verlag, 1981).

[54] L. Luo, X. Xu, L. Song, M. Zhou, Z. Zhou, H. Man, X. Wang, Y. Zhang, P. He, S. Yi, and H. Li, The Current Tension Electric Field in the Generalized Ohm's Law, *Geophysical Research Letters* **51**, e2023GL107191 (2024).

[55] A. V. Chumak, V. I. Vasyuchka, A. A. Serga, and B. Hillebrands, Magnon spintronics, *Nature Physics* **11**, 453 (2015).

[56] T. W. Speiser, Particle motion in the tail current sheet, *Advances in Space Research* **11**, 151 (1991).

[57] L. D. Landau and D. Ter-Haar, *Collected Papers of L.D. Landau* (Pergamon, Oxford, 1965).

[58] T. G. Northrop, *The Adiabatic Motion of Charged Particles*, Vol. 21 (Interscience Publishers, 1963).

[59] D. Cao, H. S. Fu, J. B. Cao, T. Y. Wang, D. B. Graham, Z. Z. Chen, F. Z. Peng, S. Y. Huang, Y. V. Khotyaintsev, M. André, C. T. Russell, B. L. Giles, P.-A. Lindqvist, R. B. Torbert, R. E. Ergun, O. Le Contel, and J. L. Burch, MMS observations of whistler waves in electron diffusion region, *Geophysical Research Letters* **44**, 3954 (2017).